Comparison of Hartree−Fock, Density Functional, Møller−Plesset Perturbation, Coupled Cluster, and Configuration Interaction Methods for the Migratory Insertion of Nitric Oxide into a Cobalt−Carbon Bond

Shuqiang Niu and Michael B. Hall*

Department of Chemistry, Texas A&M University, College Station, Texas 77843

Received: May 29, 1996; In Final Form: September 27, 1996[⊗]

Optimized geometries at the restricted Hartree−Fock (RHF), second-order Møller−Plesset perturbation (MP2), density functional theory (DFT), and configuration interaction with singles and doubles (CISD) levels are compared for the migratory insertion of NO into a Co−CH_3 σ-bond. Relative energies for these structures are examined along the reaction coordinate from the reactant (**2**) through the transition state (**TS(a)**) to the η^1-intermediate (**3**) at different levels of theory including higher levels of electron correlation such as quadratic configuration interaction with singles and doubles (QCISD), coupled cluster with singles and doubles (CCSD) and with perturbative corrections for triples (CCSD(T)), and CISD with size consistent corrections (CISD-(SCC)). DFT-B3LYP appears to give more reliable geometries in these first-row transition metal complexes than the RHF or MP2 approach. Although the MP2 optimized geometry of the product is in very good agreement with the experimental result, a near degeneracy problem affects the accuracy of the geometry optimization of the reactant, transition state, and η^1-intermediate. Because of this problem, the perturbation series (MP2, MP3, MP4) for the migratory insertion step fails to converge. Using higher level electron correlation methods such as CISD, CCSD, and QCISD are essential for energy calculations on this reaction. The CCSD//B3LYP method appears to yield the most reliable activation and reaction energies. This system is particularly sensitive to the theoretical method and would be useful as a model system for testing methods including electron correlation if better experimental values were available.

I. Introduction

It is well-known that in ab initio calculations electron correlation plays an important role and that Møller−Plesset (MP) perturbation methods[1] have given reliable results for systems involving second- and third-row transition metals.[2] However, large oscillations in the total energy difference were found in the application of perturbation theory to some reactions involving first-row transition metals.[3] During our study of the insertion of NO into a Co−CH_3 σ-bond followed by PH_3 (**1**) addition to produce the nitroso complex Co−N(O)CH_3 as shown in Chart 1, we discovered an unexpectedly large difference between the restricted Hartree−Fock (RHF) optimized geometries and second-order Møller−Plesset perturbation (MP2) optimized geometries of the reactant (**2**) and transition state (TS) for the insertion reaction (1).[4] Since the level of theory needed to obtain accurate geometries and accurate relative energies for the first-row transition metal system is only beginning to be appreciated, we undertook a more detailed examination of the early stage of this reaction.

In this work, we compare the geometries obtained at the RHF, MP2, density functional theory (DFT),[5] and configuration interaction including singles and doubles (CISD)[6] levels of theory. In addition, the relative energies of the important species are recalculated at MP3, MP4, CISD with size consistent corrections (CISD(SCC)),[6] quadratic configuration interaction including singles and doubles (QCISD), coupled cluster singles and doubles (CCSD), and perturbative corrections for triples (CCSD(T)) levels. We hope that this work will lead to a better appreciation of the problems encountered when studying first-row transition metal complexes and to further experimental and theoretical work on this sensitive system.

CHART 1

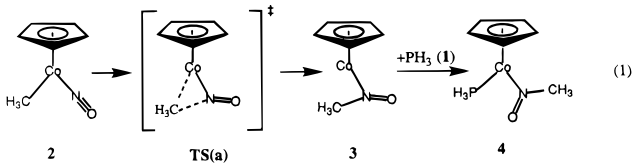

(1)

II. Computational Details

All geometries were optimized at the RHF, B3LYP, and MP2 levels. The geometries of the reactant **2** and product **4** were also optimized at the CISD level. In our ab initio calculations we replaced the phosphine group in the actual molecules by PH_3.[7] The transition states were determined and characterized by calculating the Hessian matrix. In a special case of a very small conversion barrier between two species at the MP2 level, a linear synchronous transit[8] (LST) was used for transition-state and intermediate calculations. Becke's three-parameter hybrid method[9] using the Lee−Yang−Parr correlation functional[5] (B3LYP) was employed in all DFT calculations.

For a comparison of electron correlation effects and the accuracy of calculated energies, MP2, MP3,[10] MP4SDQ,[11] CISD, CISD(SCC),[6] QCISD,[12] CCSD,[13] and CCSD(T)[14] calculations with all orbitals active were carried out with geometries optimized at the RHF, MP2, and B3LYP levels. To determine the possible multireference character of complexes, a complete active space multiconfiguration SCF (CASSCF)[15] calculation was employed in a special case.

Three different basis sets were employed in the geometry optimization, the SCF instability, and energy calculations, which are denoted as BS1, BS2, and BS3. Effective core potentials (ECPs) were used for all atoms except hydrogen. BS1 is described as the following. For cobalt, the 3s and 3p electrons

[⊗] Abstract published in *Advance ACS Abstracts,* January 1, 1997.

S1089-5639(96)01558-7 CCC: $14.00

TABLE 1: RHF, B3LYP, MP2, and CISD Fully Optimized Geometries and the Experimental Values of the Product $CpCo(N(O)CH_3)PH_3$ (4)

	RHF	DFT	MP2	CISD	expt
Co−Cp	2.076	1.849	1.731	1.888	1.718
Co−P	2.511	2.287	2.164	2.360	2.174
Co−N	1.991	1.772	1.711	1.787	1.780
N−O	1.226	1.324	1.378	1.295	1.282
N−C	1.487	1.514	1.527	1.504	1.484
P−Co−N	96.8	95.8	94.4	96.0	92.4
Co−N−O	124.2	126.4	128.3	125.4	125.6
Co−N−C	121.2	123.5	124.5	123.5	124.4
ave % dev	7.65	2.95	2.48	3.25	

were taken as active, and core potentials and basis sets were described with the double-ζ basis (541/41/41) of Hay and Wadt.[16] For carbon, nitrogen, oxygen, and phosphorus, the ECPs and basis sets of Stevens, Basch, and Krauss[17] were used in double-ζ form. [He] and [Ne] configurations were taken as cores for the first- and second-row main group atoms, respectively. The Dunning−Huzinaga (31) double-ζ basis set was used for the hydrogen atom.[18] BS2 results from BS1 by adding polarization functions[19] to all carbon, nitrogen, and oxygen atoms. BS3 results from BS1 by adding an f-type polarization function (2.70) to cobalt[20] and d-type polarization functions into oxygen, nitrogen, and carbon atoms except those in the cyclopentadienyl ring.[19]

All ab initio calculations were performed with GAMESS-UK,[21] GAUSSIAN92, and GAUSSIAN94 programs[19] at the Cornell Theory Center on IBM ES6000 and Scaleable Power-parallel (SP1 and SP2) workstations and at the Supercomputer Center of Texas A&M University on SGI Power Challenge and SGI Indigo I and II (Power Indigo) workstations in our laboratory and at the Institute Scientific Computation (ISC) of Texas A&M University.

III. Results and Discussion

A. Geometry Optimizations. First, we examine different optimization methods for obtaining geometries. The RHF/BS1, B3LYP/BS1, MP2/BS1, and CISD/BS1 fully optimized geometries of the product $CpCo(CH_3NO)PH_3$ (**4**) are given in Table 1. Compared to the experimental values of Weiner and Bergman,[22] the RHF optimized intraligand bond lengths and angles of **4** are in good agreement with the experimental values (average percentage deviation <5%), but the RHF metal−ligand bond lengths are much longer than these values (average percentage deviation 12−21%). The overall average percentage deviation is 7.65% at the RHF level. The B3LYP, MP2, and CISD geometries of **4** are in much better agreement with the X-ray structure with average percentage deviations of 2.95%, 2.48%, and 3.25%, respectively. The optimized geometry at the B3LYP level is very similar to the one at the CISD level. The largest differences between B3LYP, CISD, and MP2 values are for the Co−Cp, Co−P, and Co−N metal−ligand distances, which are all shorter at the MP2 level. Compared with the experimental values, the MP2 bond lengths for Co−Cp and Co−P are better than those of B3LYP and CISD but the MP2 value for the Co−N is worse. The short MP2 Co−N bond length and the long MP2 N−O bond length indicate that the strength of this "donation−back-donation" interaction is exaggerated by the MP2 method.

The RHF/BS1, B3LYP/BS1, MP2/BS1, CISD/BS1, MP2/BS2, and B3LYP/BS2 fully optimized geometries of the reactant $CpCo(CH_3)(NO)$ (**2**) are shown in Figure 1. Compared with the CISD optimized geometry of **2**, the RHF optimized Cp−Co, Co−NO, and N−CH_3 distances are all longer while the

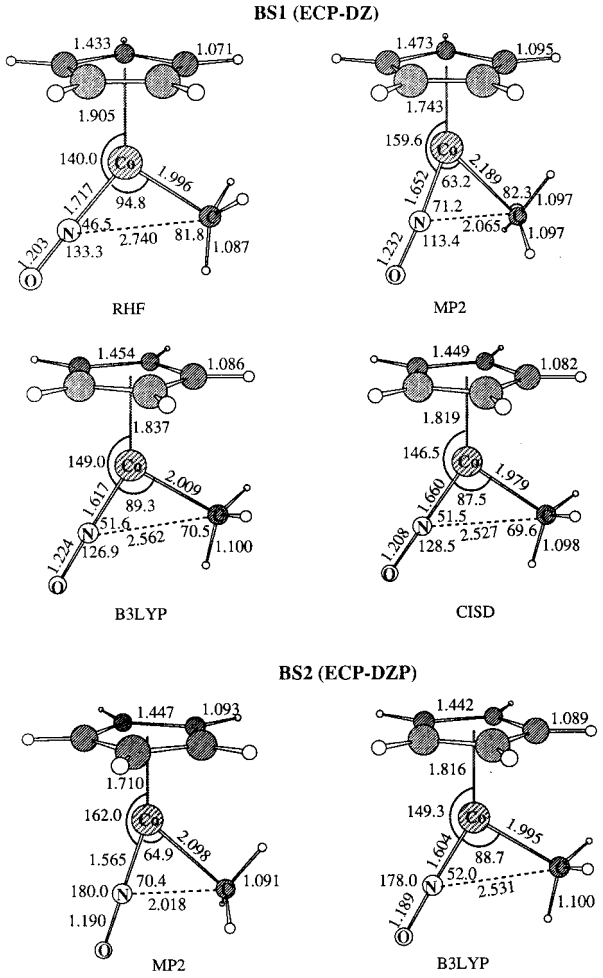

Figure 1. RHF/BS1, B3LYP/BS1, MP2/BS1, CISD/BS1, B3LYP/BS2, and MP2/BS2 fully optimized geometries of the reactant $CpCo(CH_3)(NO)$ (2)

Co−CH_3 distance is close to CISD result. The B3LYP geometry is in very good agreement with that at the CISD level; the average percent deviation is less than 2.6%. We believe that the DFT-B3LYP geometry will parallel the CISD geometry for this reaction. Therefore, we will confine the rest of this study to RHF, B3LYP, and MP2 structures. The MP2 optimized structure of **2** is both quantitatively and qualitatively different from the DFT (B3LYP) and CISD optimized ones in having a much shorter N−CH_3 distance and a rotated and distorted methyl group. Although we have no experimental data with which we can compare these results, the unusually distorted structure from the MP2 optimization is suspicious. Compared to the optimized geometries of the B3LYP/BS1 and MP2/BS1, all B3LYP/BS2 and MP2/BS2 optimized bond distances are shorter. The largest differences occur in Co−CH_3 (0.09 Å) and Co−NO (0.09 Å) bonds between the MP2/BS1 and MP2/BS2 optimized geometries. However, the angles of ON−Co−CH_3 and Cp−Co−NO are only slightly changed by BS2 at the MP2 and B3LYP levels with respect to those by BS1. The MP2 optimized geometries of **2** are very similar to the experimental structure of $[(CpMe)Co{=}N{=}O]^-$ [23] in which the angle of Cp−Co−NO and distances of the Co−NO and N−O bonds are 176.4°, 1.59 Å, and 1.23 Å. Thus, we suspect that near-degeneracy effects from an interaction between the low-lying unoccupied π^* orbitals of the NO group and high-lying occupied Co orbitals could be responsible for this MP2 geometrical distortion.[4]

To examine the absolute accuracy of these geometries, we calculated the total energies of these structures, **2**, with higher

TABLE 2: Total Energies of 2 at the CISD/BS1, CISD(SCC)/BS1, QCISD/BS1, and CCSD/BS1 Levels at the MP2/BS1, B3LYP/BS1, and CISD/BS1 Geometries

	MP2	B3LYP	CISD
CISD	−207.372 50	−207.382 18	−207.384 77
CISD(SCC)	−207.656 01	−207.654 48	−207.653 45
QCISD	−207.744 26	−207.781 70	−207.776 43
CCSD	−207.677 88	−207.705 52	−207.702 69

TABLE 3: Ten Lowest Eigenvalues (hartree) of the HF Instability Matrices with BS1 and BS2 at MP2 Equilibrium Geometry of 2

triplet		singlet	
BS1	BS2	BS1	BS2
−0.250 76	−0.247 79	0.006 40	0.014 28
−0.069 17	−0.066 53	0.016 01	0.024 82
−0.054 63	−0.060 51	0.043 32	0.045 13
−0.039 17	−0.044 45	0.058 17	0.059 72
−0.032 83	−0.040 91	0.073 49	0.071 94

level correlation methods. The total energies of **2** at the CISD/BS1, CISD(SCC)/BS1, QCISD/BS1, and CCSD/BS1 levels using the MP2/BS1, B3LYP/BS1, and CISD/BS1 geometries are shown in Table 2. At the CISD(SCC) level the MP2, B3LYP, and CISD geometries have very similar total energies. However, the B3LYP and CISD structures of **2** are more stable by 15−23 kcal/mol than the MP2 structure at the QCISD and CCSD levels. Clearly, the CISD(SCC) calculations also overestimate the stability of the MP2 geometry of **2**.

One can also check the expected performance of MP2 for this system by means of an SCF stability analysis.[24] The instability calculations of the reactant (**2**) were performed at the corresponding MP2/BS1 geometry with BS1 and BS2, respectively. The results are shown in Table 3. Not only are there five negative eigenvalues in the triplet matrices but one is very negative at about −0.25 hartree. There are no negative values in the singlet matrices in either calculation. Thus, a strong triplet instability exists, and its existence implies a strong multireference character to the reactant **2**. This near-degeneracy problem causes exaggerated contributions in the perturbation calculation. Therefore, MPX calculations may not be appropriate for this system. Furthermore, the multireference character could cause problems with other electron correlation methods. We will see examples of these problems later in this work.

The RHF/BS1 and B3LYP/BS1 fully optimized geometries of the transition state **TS(a)** and η^1-intermediate CpCo(N(O)CH_3) (**3**) are illustrated in Figure 2. The MP2/BS1 structures shown in Figure 2 are not fully optimized because the flat potential surface between **TS(a)** and **3** causes the optimization of **3** to slip smoothly to **2**. Therefore, to obtain points that are close to **3** and TS(a) at the MP2 level, we optimized a "standard" CpCo(N(O)CH_3) structure (fixing the Co−N−CH_3 angle at 120°) and then obtained a LST potential curve by linking up this structure with **2** (see Figure 4). From this curve we obtained approximate MP2 structures for **3** and **TS(a)**.

The RHF/BS1 optimized geometry of **TS(a)** is similar to the B3LYP/BS1 optimized one except for the longer N−CH_3 (the bond being formed) and, of course, a longer Co−Cp distance. The RHF and B3LYP optimized transition states have a symmetrical three-center structure, in very good agreement with the transition state of carbonyl insertion into M−R bonds.[25] In contrast, the MP2 calculated transition state has a shorter N−CH_3 and a longer Co−CH_3 distance. However, this structure is only an approximation because the suspected near-degeneracy problem that affects the geometry of the reactant (**2**) clearly affects the transition state at the MP2 level.

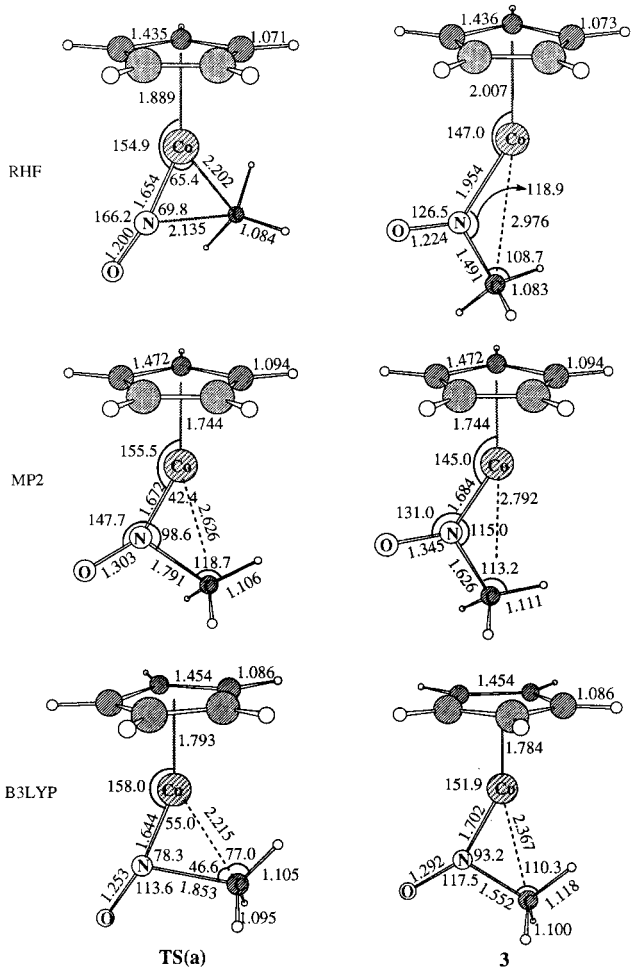

Figure 2. RHF/BS1 and B3LYP/BS1 fully optimized geometries of the transition state **TS(a)** and η^1-intermediate CpCo(N(O)CH_3) (**3**). The MP2/BS1 **3** and **TS(a)** were obtained by a LST potential curve from a "standard" CpCo(N(O)CH_3) structure (fixing the Co−N−CH_3 angle at 120°) to **2** .

The RHF/BS1 optimized geometry of the η^1-intermediate (**3**) also reveals long metal−ligand bond lengths compared with the results of the MP2/BS1 and B3LYP/BS1 calculation. The largest difference between the RHF and B3LYP optimized geometries of the η^1-intermediate (**3**) is in the Co−CH_3 distance. The B3LYP Co−N−CH_3 angle (93.2°) is obviously smaller than the normal value for sp^2 hybridization (120°). Such a structural feature points to the presence of the Co−H−C β-agostic interaction.[26] This agostic interaction is not found in the RHF geometry, which has a normal sp^2 Co−N−CH_3 angle.

In addition, it is noteworthy that the Co−Cp distances of complexes are more sensitive to changes in the electron structures of complexes at the RHF and B3LYP level than the MP2 level. The Co−Cp distances of the 18-valence electron (VE) complexes **2** and **4** are longer by about 0.05 Å than that of the 16-VE complex **3** at the B3LYP level of theory, while these distances are within 0.01 Å of each other at the MP2 level of theory.

B. Energy Determinations. The kinetic studies of Weiner and Bergman[22c] revealed the following characteristics of reaction (1): (i) the rate ($k = 1.6 \times 10^{-3}$ s^{-1} at 18 °C) does not vary as a function of PR_3; (ii) the reaction (**1** + **2** to **4**) is exothermic; (iii) the migration insertion step (**2** to **3**) is the rate-determining step of reaction. However, they do not report an activation energy. A similar migratory insertion reaction (2),

$$Mn(CO)_5CH_3 + CO \rightarrow Mn(CO)_5(C(O)CH_3) \qquad (2)$$

TABLE 4: Energies[a] at B3LYP Geometries for Various Methods with BS1 and for CCSD with BS3 for 1, 2, TS(a), 3, and 4

	1 + 2	1 + 2	1 + TS(a)	1 + 3	4
B3LYP/BS1	*−217.714 92*	0.00	10.38	7.59	−16.27
CISD//B3LYP/BS1	*−215.459 67*	0.00	0.95	−11.47	−13.61
CISD(SCC)//B3LYP/BS1	*−215.735 46*	0.00	3.30	1.54	−22.76
QCISD//B3LYP/BS1	*−215.862 24*	0.00	31.03	32.65	*b*
CCSD//B3LYP/BS1	*−215.786 06*	0.00	19.54	16.73	−9.76
CCSD/BS3//B3LYP/BS1		0.00	16.89	14.82	
CCSD(T)//B3LYP/BS1	*−215.865 20*	0.00	25.61	24.58	
CISD//CISD/BS1	*−215.462 40*	0.00			−13.33
CISD(SCC)//CISD/BS1	*−215.734 70*	0.00			−20.16

[a] Total energies (italic, in au) are given only for reactants, and relative energies (in kcal/mol) are given for other structures. [b] Fail to converge.

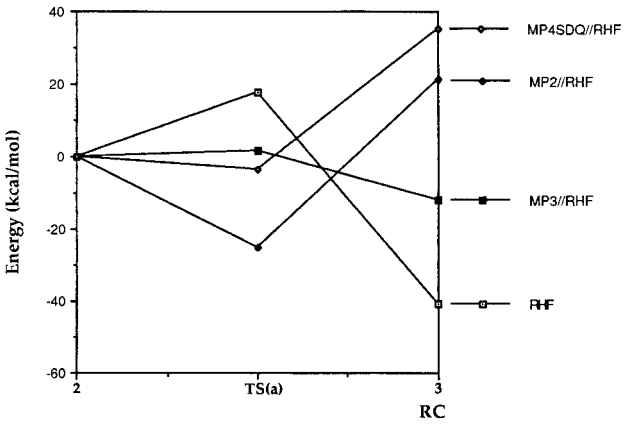

Figure 3. Relative energies obtained with BS1 for series levels of MP perturbation theory at the RHF/BS1 geometries for the reaction of **2** to **3**.

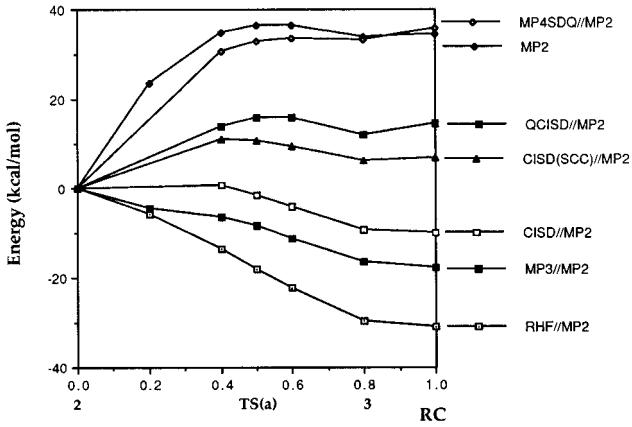

Figure 4. Relative energies obtained with BS1 for the higher perturbation series, CISD, CISD(SCC), and QCISD methods using the MP2/BS1 geometries for the reaction of **2** to **3**.

in which a CO is inserted into the Mn−CH_3 σ-bond followed by the additional CO taking up the empty coordination site, is exothermic with a reaction enthalpy of $\Delta H_2 = -13.0$ kcal/mol[27] and an activation enthalpy of $\Delta H^{\ddagger}_2 = 16.6$ kcal/mol.[28a] At 18 °C the rate constant of reaction 2, $k = 4.6 \times 10^{-4}$ s^{-1}, is only a factor of 3 less than the rate constant of reaction 1 at the same temperature. Thus, based on equations from transition state theory and the data for the rates of reactions 1 and 2,[22c,28a] the activation enthalpy $\Delta H^{\ddagger}_1$ can be estimated to be 14.5 kcal/mol.[29] By estimation of the overall enthalpy of reaction 1, ΔH_1, the stronger back-donating interaction of Co═N═O compared to Mn═C═O in the reactants and the weaker N−CH_3 bond compared to the C−CH_3 bond in the products are offset by the stronger σ-donating interaction of PR_3 compared to CO. Thus, the reaction enthalpy ΔH_1 should be close to ΔH_2, −13.0 kcal/mol. However, this latter estimate is not nearly as accurate as our estimated activation enthalpy. Furthermore, ΔH_1 will be dependent on the phosphine, which is not true of the activation enthalpy.

To obtain reliable relative energies, to examine the relative accuracy of the geometries determined above, and to determine a suitable method that accurately accounts for electron correlation effects on the total energy difference for a first-row transition metal system, we have examined relative energies along the insertion reaction path from the reactant (**2**) through the transition state (**TS(a)**) to the η^1-intermediate (**3**) as well as the reaction energy ΔE of **1** + **2** to **4** at different levels of theory (see reaction 1).

The relative energies obtained for several levels of the Møller−Plesset perturbation theory with BS1 at the RHF/BS1 geometries are shown in Figure 3. The energetic order of the reactant (**2**), the transition state (TS(a)), and the η^1-intermediate (**3**) shows substantial oscillations. Both MP2 and MP4 overestimate the stability of the RHF transition state with respect to the reactants. These severe oscillations again suggest a serious near-degeneracy problem in this system. We must conclude that the Møller−Plesset perturbation series is not sufficiently convergent for the final energy determinations.

TABLE 5: T_1 Diagnostic Values of Complexes at the CCSD/BS1//B3LYP and CCSD/BS3//B3LYP Levels

	2	TS(a)	3	4
CCSD/BS1//B3LYP	0.076			0.050
CCSD/BS3//B3LYP	0.070	0.052	0.053	

We repeated these energy calculations with BS1 at MP2/BS1 geometries and determined the energy difference by two higher-order methods, CISD and QCISD. These results are shown in Figure 4. Although MP2 and MP4//MP2 results reproduce the trend in the CISD(SCC)//MP2 and QCISD//MP2 results, they clearly overestimate the relative stability of the reactant (**2**) and transition state (**TS(a)**). Since the MP2 structure of the reactant (**2**) looks so much like the RHF structure of **TS(a)**, the expected result is that there is no barrier from **2** to **3** at the RHF//MP2 and MP3//MP2 levels.

Since we already knew that the DFT-B3LYP geometries are somewhat more accurate than the RHF and MP2 geometries, we again calculated the energetics by the higher-order methods: CISD/BS1, CISD(SCC)/BS1, QCISD/BS1, CCSD/BS1, CCSD(T)/BS1, and CCSD/BS3 at the B3LYP/BS1 geometries. Again, these results, in Figure 5, clearly show that the Møller−Plesset perturbation series for the electron correlation of this insertion reaction fails to converge. The calculated barrier at the CCSD/BS3//B3LYP level is 16.9 kcal/mol, only 2.6 kcal/mol less than that at the CCSD/BS1//B3LYP level. Thus, adding polarization functions causes only a small change in the relative energies.

The actual energies and their differences for a few of these calculations with BS1 are displayed in Table 4. The calculated

TABLE 6: Six Largest Corresponding Eigenvectors of Four-Electron Four-Orbital[a] CASSCF Calculation at the B3LYP Geometry of 2

configuration	$(12)^\alpha(12)^\beta$	$(23)^\alpha(23)^\beta$	$(13)^\alpha(24)^\beta$	$(14)^\alpha(14)^\beta$	$(12)^\alpha(34)^\beta$	$(34)^\alpha(34)^\beta$
corresponding eigenvector	0.888	−0.202	0.213	−0.290	−0.104	−0.153

[a] Occupied orbitals: d_{yz} (1), d_{xz} (2). Unoccupied orbitals: π^-_o (3), π^-_i (4) of the NO ligand. Calculated one-electron symbolic density on these orbitals are 1.81, 1.72, 0.19, and 0.28, respectively.

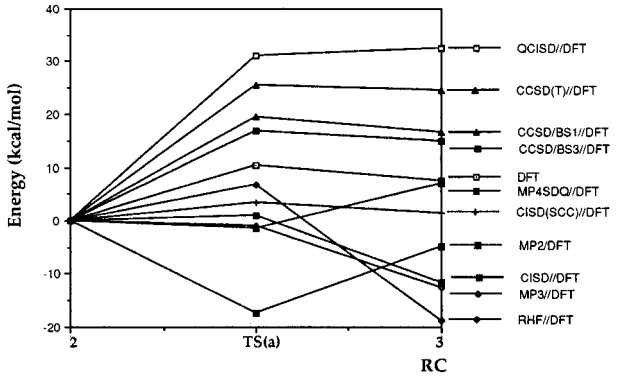

Figure 5. Relative energies obtained by the higher perturbation series, CISD/BS1, CISD(SCC)/BS1, QCISD/BS1, CCSD/BS1, CCSD(T)/BS1, and CCSD/BS3 methods, at the B3LYP/BS1 geometries for the reaction of **2** to **3**.

activation barriers of the migratory insertion step **2** → **3** at the B3LYP, CCSD/BS1//B3LYP, and CCSD/BS3//B3LYP levels are 10.4, 19.5, and 16.9 kcal/mol, respectively. Compared to our estimated experimental activation enthalpy value, 14.5 kcal/mol, the calculated barrier heights are quite reasonable, especially the CCSD value in the larger basis set. However, the calculated barrier heights at the CISD//B3LYP, CISD(SCC)//B3LYP, QCISD//B3LYP, and CCSD(T)//B3LYP levels, 1.0, 3.3, 31.0, and 25.6 kcal/mol, respectively, are outside the acceptable range, since the experimental value (estimated at 14.5 kcal/mol) could not be less than 10 or greater than 20 kcal/mol. It appears as if two correlation methods (CISD, CISD(SCC)) underestimate while two (QCISD, CCSD(T)) overestimate the correlation effects in the reactant **2**, which possesses multireference character and strong pair−pair correlation effects[30,31] because of its multiple bond Co═N═O character.

To verify the multireference character in this system, we first examine the T_1 diagnostic values of complexes (see Table 5).[30] The calculated T_1 diagnostic values of **2** are 0.076 and 0.070 at the CCSD//B3LYP/BS1 and CCSD//B3LYP/BS3 levels, respectively. The T_1 diagnostic values in BS3 for **TS(a)** and **3** are 0.52 and 0.53, respectively. Thus, **2** has a significantly larger mutireference character than **TS(a)** or **3**, and this character is independent of the basis set. Furthermore, a four-electron four-orbital CASSCF calculation at the B3LYP/BS1 geometry of **2**, where two metal orbitals, d_{yz} and d_{xz}, and two NO π orbitals, π_o^- and π_i^-, are in the active space, indicates that five doubly or quadruply excited states contribute strongly to the reference configuration state as shown in Table 6. Thus, the stronger multireference character of **2** is confirmed.

Overall, the reaction from the reactants (**1** + **2**) to product (**4**) was calculated to be exothermic with a ΔE ranging from −9.8 to −22.8 kcal/mol at the B3LYP, CISD//CISD, CISD(SCC)//CISD, and CCSD//B3LYP levels. In comparison with the estimated experimental enthalpy ($\Delta H_2 = -13.0$ kcal/mol),[27] these values appear to be fairly reasonable. However, our estimated experimental enthalpy is not nearly as reliable as the experimental activation energy. In addition, this enthalpy depends on the phosphine, which is not true of the activation energy, and previous work has shown that the nature of the phosphine can be of vital importance.[7a]

IV. Conclusion

In conclusion, the effect of electron correlation is very important for geometry optimization in first-row transition metal complexes, especially for systems with strong π-bonding ligands. DFT-B3LYP gives a much better and more reliable description of the geometries and relative energies in this first-row transition metal system than either the RHF or the MP2 approaches. Although the MP2 optimized geometry of the product is in very good agreement with the experimental result, a near-degeneracy problem affects the accuracy of the geometry optimization of the reactant, transition state, and η^1-intermediate and results in a divergence of the Møller−Plesset perturbation series for the correlation energy of the migratory insertion step. Thus, MP2 is not an appropriate method for either the geometry optimization or the correlation energy in this system. The CCSD//B3LYP method yields reasonable relative energies for this system. However, the CISD, QCISD, and CCSD(T) electron correlation methods also seem to be unsuitable for energy calculations of this system. This system appears to be particularly sensitive to the method, since near-degeneracy problems affect the accuracy of both the geometry optimizations and the final energies. This system would be particularly well suited as a model for examining a more accurate and stable electron correlation method for first-row transition metal complexes. However, additional experiment work on the system is essential.

Acknowledgment. We thank the Robert A. Welch Foundation (Grant A-648) and the National Science Foundation (Grants CHE 91-13634 and 94-23271) for financial support. This research was conducted in part with use of the Cornell Theory Center, a resource for the Center for Theory and Simulation in Science and Engineering at Cornell University, which is funded in part by the National Science Foundation, New York State, and IBM Corporation.

References and Notes

(1) (a) Møller, C.; Plesset, M. S. *Phys. Rev.* **1936**, *46*, 618. (b) Pople, J. A.; Binkley, J. S.; Seeger, R. *Int. J. Quantum Chem.* **1976**, *S10*, 1.

(2) (a) Lin, Z.; Hall, M. B. *Coord. Chem. Rev.* **1994**, *135/136*, 845. (b) Siegbahn, P. E. M.; Sevensson, M. *Chem. Phys. Lett.* **1993**, *216*, 147.

(3) (a) Masden, C. J.; Wolynec, P. P. *Inorg. Chem.* **1991**, *30*, 1681. (b) Ehlers, A. W.; Frenking, G. *J. Am. Chem. Soc.* **1994**, *116*, 1514.

(4) Niu, S.-Q.; Hall, M. B. Unpublished results.

(5) Lee, C.; Yang, W.; Parr, R. G. *Phys. Rev.* **1988**, *B37*, 785.

(6) (a) Raghavachari, K.; Pople, J. A. *Int. J. Quantum Chem.* **1981**, *20*, 1067. (b) Krishnan, R.; Schlegel, H. B.; Pople, J. A. *J. Chem. Phys.* **1980**, *72*, 4654. (c) Szabo, A.; Ostlund, N. S. *Modern Quantum Chemistry: Introduction to Advanced Electronic Structure Theory*; Macmillan Publishing Co., Inc.: New York, 1982.

(7) (a) Song, J.; Hall, M. B. *J. Am. Chem. Soc.* **1993**, *115*, 327. (b) Sulfab, Y.; Basolo, F.; Rheingold, A. L. *Organometallics* **1989**, *8*, 2139.

(8) Halgren, T. A.; Lipscomb, W. N. *Chem. Phys. Lett.* **1977**, *49* (2), 225.

(9) (a) Becke, A. D. *Phys. Rev.* **1988**, *A38*, 3098. (b) Becke, A. D. *J. Chem. Phys.* **1993**, *98*, 1372. (c) Becke, A. D. *J. Chem. Phys.* **1993**, *98*, 5648.

(10) Pople, J. A.; Binkley, J. S.; Seeger, R. *Int. J. Quantum Chem.* **1976**, *10*, 1.

(11) Krishnan, R.; Pople, J. A. *J. Chem. Phys.* **1978**, *14*, 91.

(12) Pople, J. A.; Head-Gordon, M.; Raghavachari, K. *J. Chem. Phys.* **1987**, *87*, 5968.

(13) (a) Bartlett, R. J. *Annu. Rev. Phys. Chem.* **1981**, *32*, 359. (b) Scuseria, G. E.; Schaefer, H. F., III. *J. Chem. Phys.* **1989**, *90*, 3700.

(14) Raghavachari, K.; Trucks, G. W.; Pople, J. A.; Head-Gordon, M. *Chem. Phys. Lett.* **1989**, *87*, 5968

(15) (a) Hegarty, D.; Robb, M. A. *Mol. Phys.* **1979**, *38*, 1795. (b) Schlegel, H. B.; Robb, M. A. *Chem. Phys. Lett.* **1982**, *93*, 43.

(16) Hay, P. J.; Wadt, W. R. *J. Chem. Phys.* **1985**, *82*, 299.

(17) Stevens, W. J.; Basch, H.; Krauss, M. *J. Chem. Phys.* **1984**, *81*, 6026.

(18) (a) Huzinaga, S. *J. Chem. Phys.* **1965**, *42*, 1293. (b) Dunning, T. H., Jr. *J. Chem. Phys.* **1970**, *53*, 2823.

(19) Frisch, M. J.; Trucks, G. W.; Schlegel, H. B.; Gill, P. M. W.; Johnson, B. G.; Robb, M. A.; Cheeseman, J. R.; Keith, T. A.; Petersson, G. A.; Montgomery, J. A.; Raghavachari, K.; Al-Laham, M. A.; Zakrzewski, V. G.; Ortiz, J. V.; Foresman, J. B.; Cioslowski, J.; Stefanov, B. B.; Nanayakkara, A.; Challacombe, M.; Peng, C. Y.; Ayala, P. Y.; Chen, W.; Wong, M. W.; Andres, J. L.; Replogle, E. S.; Gomperts, R.; Martin, R. L.; Fox, D. J.; Binkley, J. S.; Defrees, D. J.; Baker, J.; Stewart, J. P.; Head-Gordon, M.; Gonzalez, C.; Pople, J. A. *Gaussian 94*, Revision A.1; Gaussian, Inc.: Pittsburgh, PA, 1995.

(20) The f-type polarization function, 2.70, was optimized for Co−N−O at the CISD//B3LYP level.

(21) Guest, M. F.; Kendrick, J.; van Lenthe, J. H.; Schoeffel, K.; Sherwood, P. *GAMESS-UK*; Daresbury Labratory: Warrington, U.K.

(22) (a) Weiner, W. P.; White, M. A.; Bergman, R. G. *J. Am. Chem. Soc.* **1981**, *103*, 3, 3612. (b) Seidler, M. D.; Bergman, R. G. *Organometallics* **1983**, *2*, 1897. (c) Weiner, W. P.; Bergman, R. G. *J. Am. Chem. Soc.* **1983**, *105*, 3922.

(23) Weiner, W. P.; Hollander, F. J.; Bergman, R. G. *J. Am. Chem. Soc.* **1984**, *106*, 7462.

(24) (a) Kawamura-Kuribayashi, H.; Koga, N.; Morokuma, K. *J. Am. Chem. Soc.* **1992**, *114*, 2359. (b) Weiss, H.; Ehrig, M.; Ahlrichs, R. *J. Am. Chem. Soc.* **1994**, *116*, 4919.

(25) (a) Koga, N.; Morokuma, K. *Chem. Rev. (Washington, D.C.)* **1991**, *91*, 823. (b) Axe, F. U.; Marynick, D. S. *J. Am. Chem. Soc.* **1988**, *110*, 3728. (c) Ziegler, T.; Versluis, L.; Tschinke, V. *J. Am. Chem. Soc.* **1986**, *108*, 612.

(26) (a) Dwoodi, Z.; Green, M. L. H.; Mtetwa, V. S. B.; Prout, K.; Schultz, A. J.; Williams, J. M.; Koetzle, T. F. *J. Chem. Soc., Dalton Trans.* **1986**, *802*, 1629. (b) Dwoodi, Z.; Green, M. L. H.; Mtetwa, V. S. B.; Prout, K. *J. Chem. Soc., Chem. Commun.* **1982**, *802*, 1410.

(27) Connor, J. A.; Zafarani-Moattar, M. T.; Bickerton, J.; Saied, N. I. E.; Suradi, S.; Carson, R.; Al Takhin, G.; Skinner, H. A. *Organometallics* **1982**, *1*, 1166.

(28) (a) Butler, I. S.; Basolo, F.; Pearson, R. G. *Inorg. Chem.* **1967**, *6*, 2074. (b) Green, M.; Westlake, D. J. *J. Chem. Soc. A* **1971**, 367.

(29) Here, we suppose that the pre-exponential factor and the activation entropy are the same for these insertion reactions. Although one might be skeptical of this assumption, we can check this method by estimating the activation enthalpy of $CpFe(CH_3)(CO)_2$ to $CpFe(CO)(C(O)CH_3)$. Using this method, we estimate $\Delta H^{\ddagger}$ for this insertion to be 21.3 kcal/mol, a value that is in very good agreement with the experiment values 18.2 [28b] and 26.1 [28a] (average 22 kcal/mol).

(30) Lee, T. J.; Scuseria, G. E. *Quantum Mechanical Electronic Structure Calculations with Chemical Accuracy*; Langhoff, S. R., Ed.; Kluwer Academic Publishers: Dordrecht, 1995; pp 47−108.

(31) He, Z.; Kraka, E.; Cremer, D. *Int. J. Quantum Chem.* **1996**, *57*, 157.